Carbohydrate Research, 107 (1982) 17–32
Elsevier Scientific Publishing Company, Amsterdam – Printed in The Netherlands

VISCOSITY–MOLECULAR WEIGHT RELATIONSHIPS, INTRINSIC CHAIN FLEXIBILITY, AND DYNAMIC SOLUTION PROPERTIES OF GUAR GALACTOMANNAN

GEOFFREY ROBINSON, SIMON B. ROSS-MURPHY*, AND EDWIN R. MORRIS
Unilever Research, Colworth Laboratory, Sharnbrook, Bedford MK44 1LQ (Great Britain)
(Received February 8th, 1982; accepted for publication, February 15th, 1982)

ABSTRACT

Molecular theories of the viscosity of dilute and more concentrated solutions of random-coil polymers have been applied to five molecular-weight fractions of guar galactomannan. The variation in intrinsic viscosity ($[\eta]$; $dL.g^{-1}$) with molecular weight (M_r) followed the relationship $[\eta] = 3.8 \times 10^{-4} M_r^{0.723}$, consistent with random-coil behaviour. The intrinsic stiffness of the galactomannan backbone was estimated by evaluating the "characteristic ratio" C_∞, which is ~ 12.6 and agrees well with results for carboxymethylcellulose, which has a closely similar, β-(1→4)-linked polymer backbone. At intermediate concentrations (c), up to specific viscosities of ~ 10, η_{sp} was proportional to $c^{1.3}$, while at higher concentrations, η_{sp} was $\sim c^{5.1}$. This exponent is higher than is usually observed for polymers interacting purely by physical entanglement, and is evidence for more specific polymer–polymer interactions ("hyperentanglements"). The concentration dependence and the time-scale of entanglement coupling have been monitored by both steady-shear and oscillatory measurements, and a generality of response has been demonstrated.

INTRODUCTION

Galactomannans are water-soluble polysaccharides found in the seed endosperm of a variety of legumes, and consist of a (1→4)-linked β-D-mannopyranosyl backbone partially substituted at O-6 with α-D-galactopyranosyl side-groups[1]. Guar and locust bean (carob) galactomannans are widely used as industrial hydrocolloids[2], principally because they impart high viscosity at relatively low concentrations. The gums from different sources usually vary in, for example, mannose/galactose ratio, distribution of galactose residues along the mannan backbone, molecular weight, and molecular weight distribution.

Recent papers[3–6] have considered the solution properties of galactomannans, and particularly of guar gum, either to relate such molecular properties as molecular weight and intrinsic viscosity to the properties of dilute solutions, or alternatively

*To whom correspondence should be addressed.

0008-6215/82/0000–0000/$ 02.75,

to examine flow behaviour at higher concentrations in terms of phenomenological models. We consider here flow behaviour over the entire regime of industrial interest, using the molecular treatments which have been widely applied to synthetic polymer solutions and melts over the last fifteen years[7,8]. A number of revealing generalities of behaviour are observed, and the results obtained for five guar fractions of different chainlength can be rationalised in molecular terms, and are consistent with previous work from this laboratory on a range of other polysaccharides[9–11].

EXPERIMENTAL

Materials. — Five grades of commercial guar gum [Vidocrem samples A, B, C, D, and F (Unipektin A.G., Switzerland)] were purified by dissolving in deionised water and then recovering each sample by ethanol precipitation. A solution of each precipitate in water was then freeze-dried. Absolute concentrations of galactomannan in the freeze-dried materials were determined by elemental analysis (Butterworth Microanalytical Consultancy Ltd., U.K.). Relative proportions of mannose and galactose were determined by acid hydrolysis, and g.l.c. of the resulting monosaccharides as alditol acetates. For each sample, the ratio of galactose to mannose was 0.64 $\pm$0.02, thus raising the effective molecular weight per backbone residue from 162 for unsubstituted mannan to 266 (162 × 1.64). Solutions were prepared by dissolving known weights of the dry sample in deionised water. For studies by light scattering and dilute solution viscosity, samples were also extensively dialysed and the final concentrations determined by phenol–sulphuric acid assay[12].

Dilute solution viscometry ($\eta_r < 25$). — The shear viscosity of a liquid is the ratio of stress (τ) to the rate of shear ($\dot{\gamma}$), where $\dot{\gamma}$ depends upon the geometry of the viscometer and, for example, for a concentric cylinder apparatus, is given by the approximate relationship shown in Eq. *1*.

$$\dot{\gamma} \approx \Omega r_1/(r_2 - r_1), \qquad (1)$$

where r_1 and r_2 are the radii of the inner and outer cylinders, and Ω is the rotational velocity (rad.s^{-1}).

For most polymer solutions, the dependence of viscosity upon shear rate is as illustrated in Fig. 1; they are shear thinning and, even for dilute solutions, measurements should be made at a number of different shear rates so that η_0, the "zero shear viscosity", can be established.

The viscosities of dilute solutions of guar gum were determined by using a low-shear (shear-rate range, 1–30 s^{-1}), coaxial cylinder apparatus similar to that described by Ogston and Stanier[13]. Intrinsic viscosities [η] were determined for each solution by measuring relative viscosities ($\eta_r = \eta/\eta_s$, where η is the viscosity of the solution, and η_s that of the solvent) over the range $1.2 < \eta_r < 2.0$, and over the full range of available shear rates. Even such dilute solutions (typically <0.2% w/w) can be "shear thinning"[8,9], so that the usual capillary viscometer (shear rate$\approx$ 200 s^{-1}) should be used with caution. By the present method, shear-rate independence

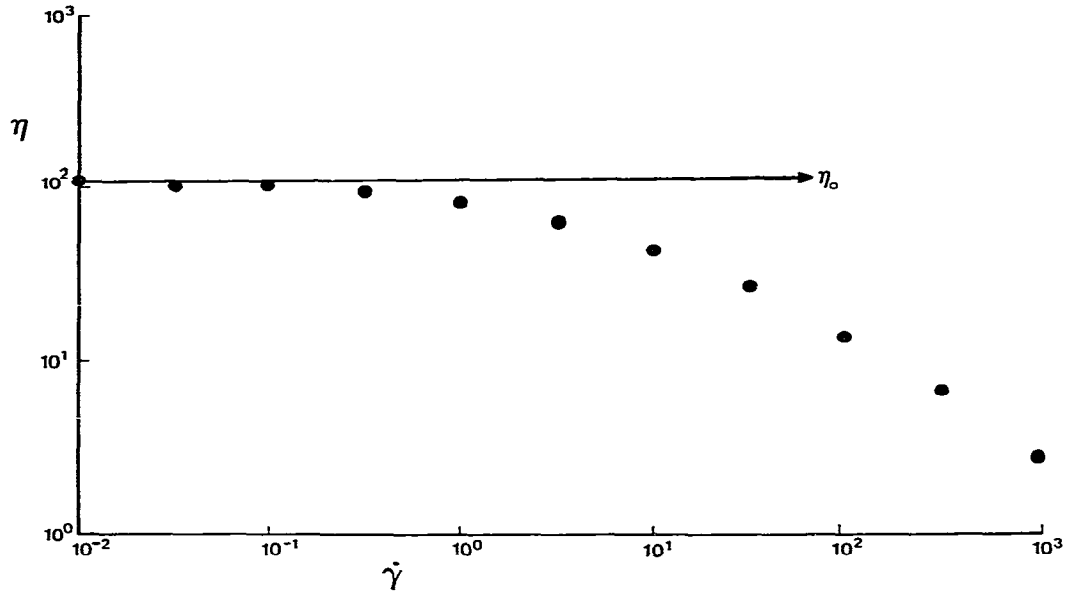

Fig. 1. Shear-rate ($\dot{\gamma}$) dependence of viscosity (η), illustrated as a double-logarithmic plot for Vidocrem C (2% w/v). The maximum, constant value of η attained at low rates of shear is the "zero shear" viscosity (η_0).

can be verified directly, and the "zero shear" intrinsic viscosity determined[9] by the usual Huggins (Eq. *3*) and Kramer (Eq. *4*) extrapolations.

$$\eta_{sp} = \eta_r - 1 \tag{2}$$

$$\eta_{sp}/c = [\eta] + k'[\eta]c^2 \tag{3}$$

$$\ln(\eta_r)/c = [\eta] + k''[\eta]^2 c \tag{4}$$

This same apparatus, fitted with a less-sensitive torsion wire, was also used for relative viscosities up to ~25. Since, for water, η_s is 0.89 mPa.s at 25°, this corresponds to actual viscosities of ~20 mPa.s (or, in older units, ~20 cP).

Viscosity at higher concentrations ($10 < \eta_r < 6 \times 10^5$). — At polymer concentrations such that η_r is greater than 10 (*i.e.*, $\eta \gtrsim 10$ mPa.s), the effect of shear rate becomes even more important, so that an instrument capable of measuring over a wide range of shear rates is essential. Most such measurements are performed with a "cone and plate" instrument, because this has the advantage of providing a homogeneous shear rate throughout the sample. Our experiments were performed by using a Rheometrics Mechanical Spectrometer RMS-605 (Rheometrics Inc., Union, NJ, U.S.A.) with automatic computation and plotting of results. Both sensitive (ST-10) and normal (TC-2000) transducers were used, together with cone and plate assemblies having cone angles θ of 0.1 and 0.04 rad. In the cone and plate configuration, shear rate $\dot{\gamma}$ is given by Eq. *5*.

$$\dot{\gamma} = \Omega/\theta, \tag{5}$$

where Ω is the rotational velocity of the cone relative to the plate (rad.s^{-1}). In practice, the instrument could be used over the shear-rate range from 10^{-2} to 2.5×10^{3} s^{-1}, and the shear-rate dependence of solution viscosity was measured for each sample over the concentration range 1–3% w/w.

Mechanical spectrometry. — The Rheometrics instrument can also be used to measure the response of solutions to oscillatory shear. If a sinusoidal shear is applied to a perfect solid, the resultant stress is exactly in phase, whereas the stress is 90° out of phase for a perfect liquid. Polymer solutions show intermediate behaviour (viscoelasticity)[8], having an element of both solid-like character (measured as the in-phase component of the resultant stress) and liquid-like character (measured as the out-of-phase component). The ratio of in-phase stress to amount of shear is the storage modulus G′, and G″, the loss modulus, is the ratio of out-of-phase stress to shear. Both G′ and G″ can be charted as a function of oscillatory frequency, ω.

Light-scattering measurements. — Wide-angle light-scattering measurements were made on a commercial Sofica photometer (42000), using vertically polarised, blue light (λ = 436 nm). The solutions were dialysed against solvent, and dilutions made using the dialysate, to minimise distortion of the concentration dependence of scattered-light intensity by thermodynamic effects[14]. In further studies, the guar samples were dissolved in 8M urea, and then dialysed to give a final urea concentration of 0.1M. Low-angle measurements of scattered-light intensity were made with the Chromatix KMX-6 laser light-scattering instrument (λ = 633 nm). The differential refractive-index increment dn/dc was determined at 633 nm with a Chromatix KMX-16 laser differential refractometer, and was 0.135 mL.g^{-1} for the sample in water, and 0.129 mL.g^{-1} for the sample in 0.1M urea. The increment dn/dc was also measured with a Waters R403 differential refractometer (incandescent light source) and was 0.140 mL.g^{-1}. The wavelength dependence and the value of dn/dc in water are similar to those reported for other neutral polysaccharides[15,16]. Using both photometers, measurements of the angular dependence of scattered light could be made over a wide range of the "scattering vector" $\mathbf{k}$ [$= 4\pi/\lambda'\sin(\vartheta/2)$], from 1.2×10^{6} m^{-1} to 4.2×10^{-7} m^{-1} (where $\lambda' = \lambda/n_0$; n_0 is the refractive index of the solvent, measured at wavelength λ). Molecular weights were determined both by graphical and computational analysis using the generalised Zimm method[17].

RESULTS AND DISCUSSION

Light scattering. — The weight-average molecular weight $\overline{M}_w$ of a polymer sample can be determined from light-scattering data, using Eq. *6*.

$$(Kc/R_\vartheta)_{\vartheta=0,c=0} = 1/\overline{M}_w, \qquad (6)$$

where K is an optical constant, c is concentration, R_ϑ is the Rayleigh ratio of the excess scattered-light intensity at scattering angle ϑ, and this expression is extrapolated to zero scattering angle and zero concentration. This extrapolation procedure is the basis of the "Zimm plot" method, illustrated in Fig. 2 for Vidocrem C. However,

caution must be exercised in making this extrapolation, particularly for water-soluble polymers, because of various anomalies. (1) The concentration dependence of scattered-light intensity is not always linear; in some cases, the slope of this line (Fig. 2) is so high that the intercept on the Kc/R_ϑ axis is uncertain. (2) For many water-soluble polymers, including polysaccharides, it is often difficult to obtain complete molecular dispersion in solution, *i.e.*, "the solutions contain in addition to individual macromolecules also supermolecular particles"[18]. Kratochvíl[18] points out that even a very small amount of such material can distort the angular dependence of scattered light in a quite characteristic fashion, producing a pronounced downturn in these data, and indicating a much higher $\overline{M}_w$ than is reasonable for the particular sample. Evidence of such behaviour in solutions of guar galactomannans is shown in Fig. 3, where low-angle and wide-angle measurements on the same sample are directly compared.

This effect has several consequences that are important for the present study[18]. (1) The particles of very high molecular weight, although present in relatively small numbers, can lead to a disproportionate increase in the overall weight-average molecular weight from light scattering. (2) These supermolecular particles usually cannot be completely removed from the solution by normal procedures (filtration,

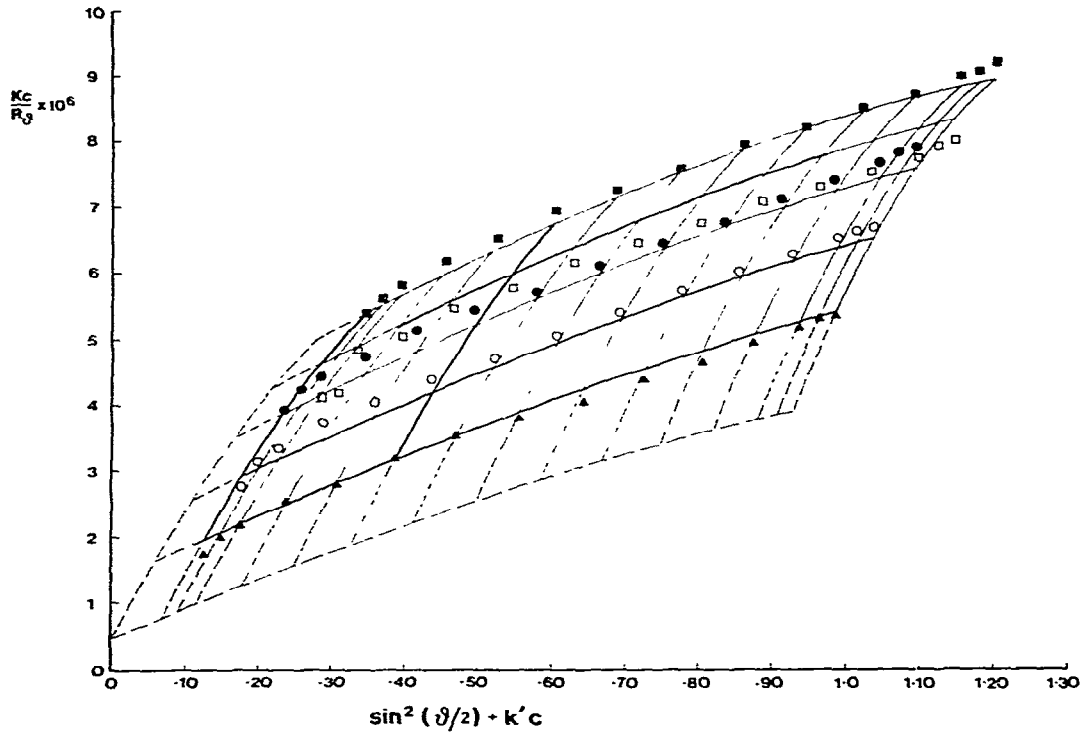

Fig. 2. Computed Zimm plot for Vidocrem C. Light-scattering data (λ = 436 nm) were obtained at the following (nominal) polymer concentrations: 0.5 (—■—); 0.4 (—□—); 0.3 (—●—); 0.2 (—○—), and 0.1% w/v (—▲—).

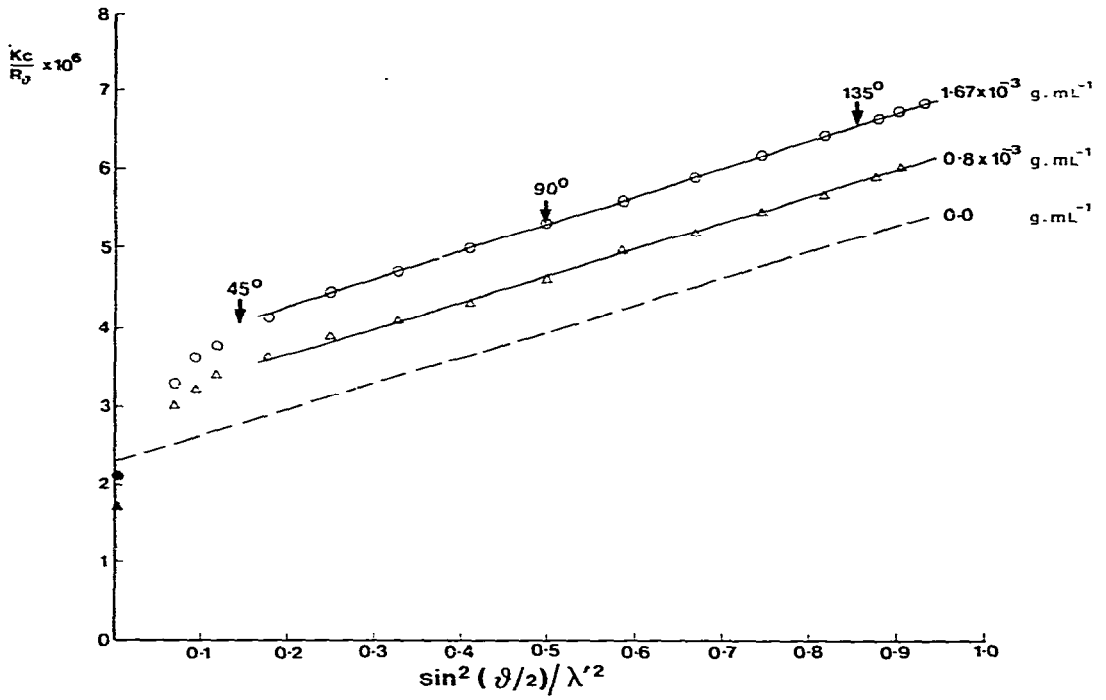

Fig. 3. Angular dependence of scattered-light intensity, illustrated for Vidocrem A: open symbols, Sofica data (blue light; $\lambda = 436$ nm; $\lambda' = \lambda/n_0 = 327$ nm); filled symbols, Chromatix data (red light; $\lambda = 633$ nm; $\lambda' = 475$ nm); concentrations as indicated.

centrifugation), and the experiment must therefore be performed in their presence. (3) The supermolecular particles, although of high molecular weight, usually have an extremely compact, spherical shape, and thus their contribution to the intrinsic viscosity of the sample is slight. (4) Estimates of the molecular size of the polymer (*e.g.*, mean-square radius of gyration) from the angular dependence of scattered light are liable to be highly unreliable.

To overcome these problems, two techniques may be adopted. First, that used by several authors, including Kratochvíl, to analyse the data at decreasing scattering angles, until the first datum is encountered which falls below the straight-line extrapolation from the higher angles. Typically, this may require the data at scattering angles below (say) 50° to be ignored. This is a technique which is useful and may be theoretically justified, although caution must be exercised in its application. An extended justification for the strategy of restricting attention to the high-angle data has been presented by Jordan and Brant[19] for the light scattering of amylose. The technique has been applied[20,21] to other polysaccharides and to some synthetic polymer systems.

Alternatively, chemical methods may be used to eliminate the aggregation. For example, non-covalent intermolecular association may be disrupted either by chemical modification of the polymer, or by use of a "denaturant" such as urea. The latter

TABLE I

MOLECULAR WEIGHTS AND INTRINSIC VISCOSITIES

Sample	$\bar{M}_w \times 10^{-5}$	$[\eta]$ *(dL.g^{-1})*
A	4.4	4.5
B	5.1	5.0
C	7.9	6.5
D	11.2	8.8
F	16.5	12.5

method has been applied in a recent *dynamic* light-scattering study of the aggregation of xanthan gum in dilute solution[22]. Unfortunately, in our experience, the high concentration (4M) of urea used by the above workers is unsuitable for *static* light-scattering measurements such as are described here, and we have used only 0.1M urea solutions. This had the effect of partially reducing the "angular downturn" of Figs. 2 and 3, while the intrinsic viscosities were, within experimental error, the same as those in aqueous solution.

Dilute solution viscosity. — The measured intrinsic viscosities of the five samples studied are given in Table I, together with the molecular weights from the light-scattering studies described above. According to the Mark–Houwink relationship (Eq. *7*), polymer intrinsic viscosity varies with molecular weight such that

$$[\eta] = K' M_r^{\alpha}, \qquad (7)$$

where the two parameters K' and α are both related to the "stiffness" of the polymer. In particular, if the polymer is a rod, then α is ~ 1.8, whereas, for a "random flight" flexible coil, it is usually assumed to lie in the range 0.5–0.8 (although a recent calculation by Daoud and Jannink[23] indicates an upper limit of 0.74). Alternatively, if the polymer adopts a very compact conformation in solution, either because it is highly branched or because of intramolecular segment–segment attractions, then α is usually small (0.1–0.3). Both K' and α can be determined directly from a double-logarithmic plot of $[\eta]$ against M_r. Analysis of our results in this way (Fig. 4) gives $\alpha = 0.723$ and $K' = 3.8 \times 10^{-4}$ dL.g^{-1}. In Fig. 4, data published by two other groups of workers are also shown, together with lines to represent their best estimates for K' and α. Results by Sharman and co-workers[5] give a slope (0.80) similar to ours, but with a significantly higher K'. We suggest that this may arise from an unusual method for the determination of intrinsic viscosity, involving a logarithmic extrapolation from viscosities measured in relatively concentrated solutions, rather than the conventional extrapolations from very dilute solutions (Eqs. *3* and *4*). The other data, by Doublier and Launay[3,4], lie quite close to our own, but with a somewhat steeper slope ($\alpha \sim 0.98$), leading to a significantly lower value of K'.

The above evidence indicates that, under the conditions of our work, guar galactomannan acts as a random-coil polymer, and that we can use one of the methods

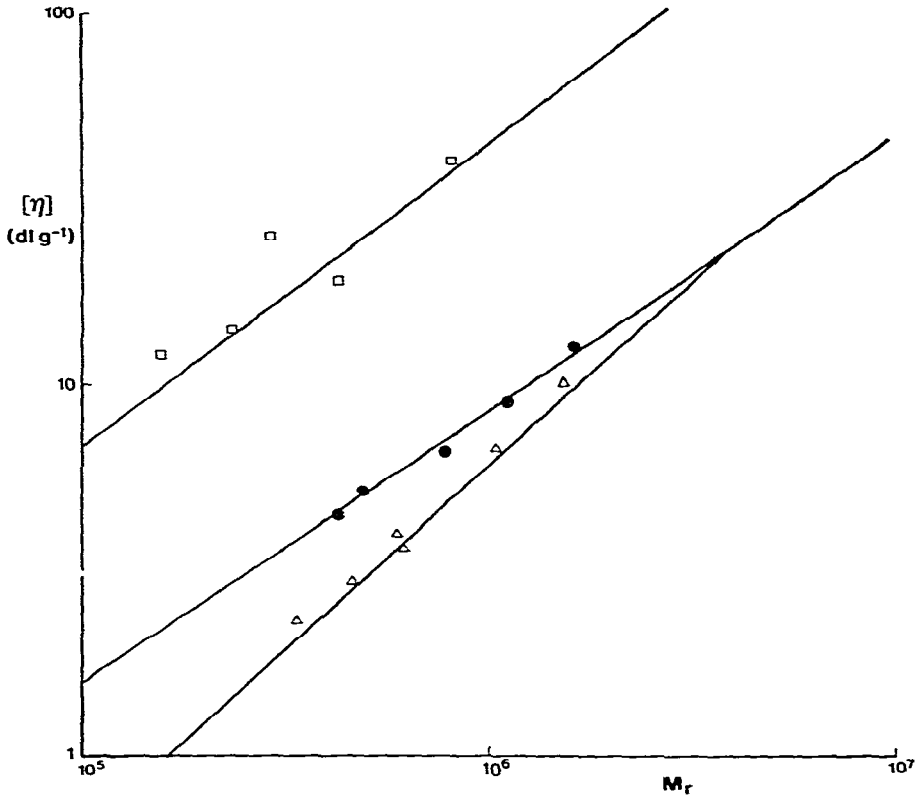

Fig. 4. Variation in intrinsic viscosity ([η]) of guar galactomannan with relative molecular mass (M_r), shown as a double-logarithmic Mark–Houwink plot (Eq. 7). Data obtained in the present work (—●—) are compared with results reported by Doublier and Launay[4] (—△—) and by Sharman and co-workers[5] (—□—).

commonly employed in synthetic polymer studies, and also applied to a limited extent to polysaccharide systems (for example, for hyaluronic acid[24]), to calculate the intrinsic chain flexibility.

Determination of intrinsic chain flexibility: the characteristic ratio (C_∞). — The simplest description of a linear polymer in dilute solution is the "random flight" model, in which the chain is considered as a collection of stiff rods connected by totally flexible, universal joints. If the number of rods is n, and each is of length l, then the average ("root mean square") distance L' between the two chain ends is given by Eq. 8.

$$L' = n^{\frac{1}{2}} l \tag{8}$$

In practice, measured values of end-to-end distance (L) are nearly always greater than L', for two main reasons. Firstly, rotation about inter-residue bonds is normally restricted to a small proportion of conformational space, *i.e.*, most combinations of the dihedral angles (ϕ, ψ) between adjacent residues (Fig. 5) are sterically or energetically disallowed, and the chain is more "directed" than in the random

flight model. At the same time, the random flight treatment neglects the "excluded volume" effect[25], namely, that two segments a distance apart along the chain backbone cannot physically occupy the same volume of space. Both of these factors increase the overall end-to-end distance, but only the first describes the intrinsic chain flexibility. However, as the molecular weight of the polymer (and thus n, the number of residues) is decreased, the excluded volume effect becomes smaller, and Eq. *9* can be written for the ratio C_∞, the "characteristic ratio" of the chain.

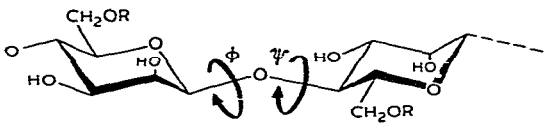

I

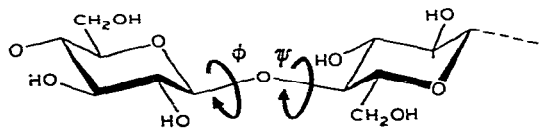

II

Fig. 5. Comparison of the primary structure of guar galactomannan (I; R = H in some residues, and α-D-galactosyl in others) with cellulose (II). The polymer backbones differ only in configuration at C-2. Overall chain conformation is determined by the dihedral angles ϕ and ψ at each inter-residue linkage.

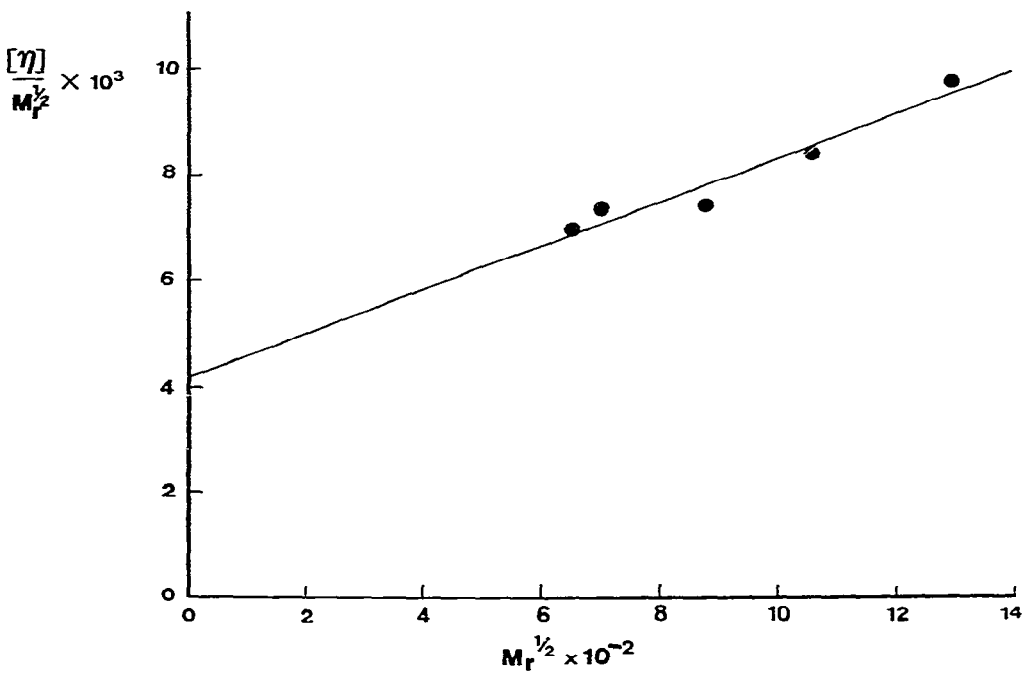

Fig. 6. Stockmayer–Fixman plot ($[\eta]/M_r^{\frac{1}{2}}$ *vs.* $M_r^{\frac{1}{2}}$) for the five Vidocrem samples studied.

$$C_\infty = L^2/L'^2, \tag{9}$$

where the characteristic ratio reflects only the local conformational freedom, or the intrinsic chain flexibility.

Under the conditions where excluded volume may be neglected, intrinsic viscosity, molecular weight, and L' may be related by the Flory–Fox equation (Eq. *10*),

$$[\eta] = \Phi L^3/M_r, \tag{10}$$

where Φ is a constant ($\sim 2.5 \times 10^{26}$ kg^{-1}). It follows from Eqs. *8* and *9* that

$$L^2 = C_\infty l^2 M_r/m, \tag{11}$$

where M_r/m ($= n$) is the ratio of the polymer molecular weight to the residue molecular weight (m), and hence (Eqs. *10* and *11*) that

$$[\eta] = \Phi l^3 (C_\infty/m)^{3/2} M_r^{\frac{1}{2}} = K_\theta M_r^{\frac{1}{2}}. \tag{12}$$

Experimentally, the characteristic ratio can be obtained (Eq. *12*) by plotting $[\eta]M_r^{\frac{1}{2}}$ against $M_r^{\frac{1}{2}}$, when the intercept is equal to K_θ. This strategy[26,27] (known as a Stockmayer–Fixman plot) is shown in Fig. 6 for the samples studied.

K_θ is 4.2×10^{-4} m^3.kg^{-1} which, using[9] $l = 0.54$ nm and $m = 266$, gives a value for C_∞ of 12.6 (± 1.5). This is fully consistent with the value (14.2) of C_∞ calculated from data reported[28] for carboxymethylcellulose, since both polymers have a diequatorial, (1→4)-linked backbone structure (Fig. 5) differing only in the configuration at C-2. The axial orientation of O-2 in the mannan chain, however, would be expected[29] to allow somewhat greater conformational freedom at each glycosidic linkage, leading, as observed, to a lower characteristic ratio. Stockmayer has recently reemphasised[30] that the technique should not be used for polymers which are known (perhaps from other evidence) to be intrinsically very stiff, or where the exponent (α) in the Mark–Houwink equation (Eq. *7*) is significantly greater than 0.8. For these stiffened coils (or "wormlike chains"), other treatments[31–33] should be used.

Solution behaviour at higher concentrations. — The above discussion has been confined to extremely dilute solutions, where individual polymer coils are spatially

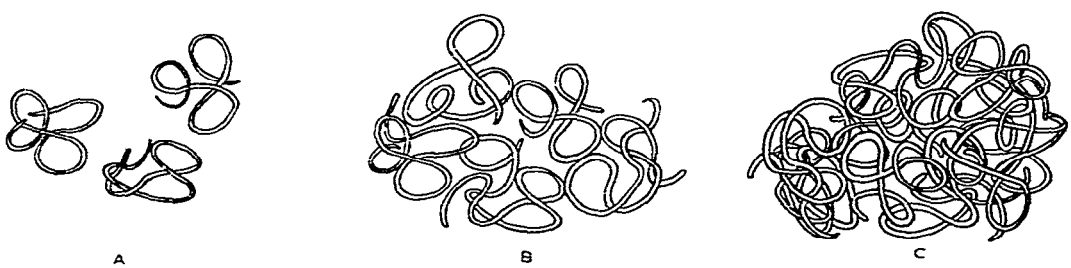

Fig. 7. Illustration of different concentration regimes: A, dilute solution (individual molecules) ($c < c^*$); B, molecules showing incipient overlap ($c \approx c^*$); C, uniform polymer-segment concentration ($c > c^*$).

separated. As the concentration of polymer is increased, the individual molecules are brought into contact with one another (Fig. 7); this is accompanied by a dramatic change in flow behaviour and, in particular, by a sudden increase in the concentration-dependence of zero-shear viscosity.

The concentration (c*) at which this occurs is inversely related to the volume occupied by the isolated polymer coils[7,8,34]. For a range of different disordered polysaccharides, it has been shown that

$$c^* \approx 4/[\eta], \tag{13}$$

where the units of $[\eta]$ are reciprocal concentration. One consequence of this generality of behaviour is that viscosity data for different concentrations and different molecular

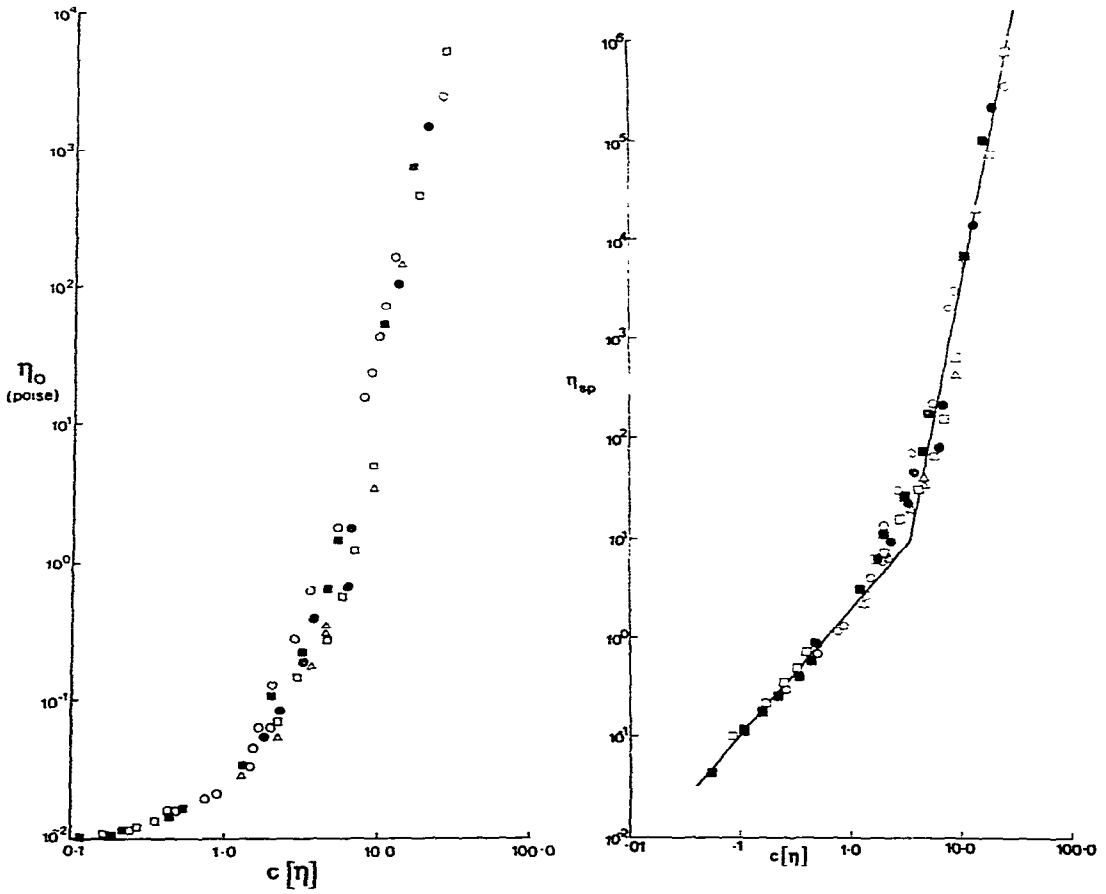

Fig. 8. Variation of "zero shear" viscosity (η_0) with degree of coil overlap, characterised by $c[\eta]$. Results are shown as a double-logarithmic plot for Vidocrem samples A (△), B (■), C (●), D (□), and F (○).

Fig. 9. Variation of specific viscosity (η_{sp}), measured at "zero shear", with coil overlap ($c[\eta]$). Presentation of results in this way avoids the compression of viscosity data at low concentrations (*cf.* Fig. 8); symbols as in Fig. 8.

weights may be plotted in a suitable reduced form, and a master plot obtained[7,11]. In Fig. 8, values of η_0 are plotted logarithmically against $c[\eta]$; above $c[\eta] \approx 4$, this plot has a slope of 5.1, whereas at $c[\eta] < 4$, the slope is much less. These results are in good agreement with work on many synthetic polymers and disordered polysaccharides, except that the slope of 5.1 is higher than was found for linear polymers interacting by purely topological entanglements, and by space-filling considerations. For example, De Gennes[34] has predicted that, for this effect of physical entanglement, $\eta_0 \sim M^3c^{3.75}$ when $c > c^*$. In Fig. 9, values of η_{sp} are plotted against the same ordinate as in Fig. 8, but the dilute-solution behaviour can more easily be established. For $\eta_{sp} < 10$, $\eta_{sp} \sim c^{1.3}$, a value which agrees well with that observed for a range of other polysaccharides[11], whereas, at $c > c^*$, $\eta_{sp} \sim c^{5.1}$, which is a little higher than predicted. This behaviour has been attributed[11] to the occurrence, in addition to normal topological entanglement, of specific interactions ("hyperentanglements")[35] between chain segments.

At the same time, a master curve appropriate for the entire range of experimentally obtainable shear rates has been derived from the assumption that the shear-rate dependence of viscosity is caused by a progressive decrease in the steady-state entanglement density. For a polymer of known molecular weight and intrinsic viscosity, a relaxation time t can be defined as[7,8]

$$t = 6\,\eta_s[\eta]M_r/\pi^2RT, \tag{14}$$

where R is the Gas Constant, T is the absolute temperature, and the constant $6/\pi^2$ is derived from the Rouse (bead-spring) model of polymer dynamics[25].

For finite concentrations, $[\eta]$ is replaced by $(\eta_0 - \eta_s)/\eta_s c$ (*cf.* Eq. *3*), and thus

$$t = 6(\eta_0 - \eta_s)M_r/\pi^2 cRT. \tag{15}$$

The relative magnitude of the imposed time-scale (*i.e.*, shear rate, $\dot{\gamma}$) and the time-scale of Eq. *15* can be expressed (Eq. *16*) in terms of a dimensionless parameter $\beta = (t\dot{\gamma})\pi^2/6$, known as the "generalised shear rate".

$$\beta = \dot{\gamma}(\eta_0 - \eta_s)M_r/cRT \tag{16}$$

If the extent of shear thinning (*i.e.*, η/η_0) at a given shear rate were to be plotted against the corresponding value of β, then, knowing η_0, M_r, c, and T, we would hope to superpose all the viscosity/shear rate data, for all concentrations and molecular weights. The plot corresponding to the Vidocrem guar solutions is given as Fig. 10, and the superposition is remarkably good. The limiting slope of this plot is ~ -0.79, which compares quite well with the value of $-9/11$ (-0.818) predicted from the theory of Graessley for monodisperse polymers[36]. With increasing polydispersity of chainlength, a reduction in terminal slope down to a limiting value of ~ -0.74 is predicted theoretically[36], and has been verified experimentally.

In Fig. 11, the moduli G′ (storage; solid-like) and G″ (loss; liquid-like) for 1%, 2%, and 3% solutions of Vidocrem D are plotted against frequency (ω). For the 2% solution at low frequencies, $G'' > G'$, and so the solution is predominantly

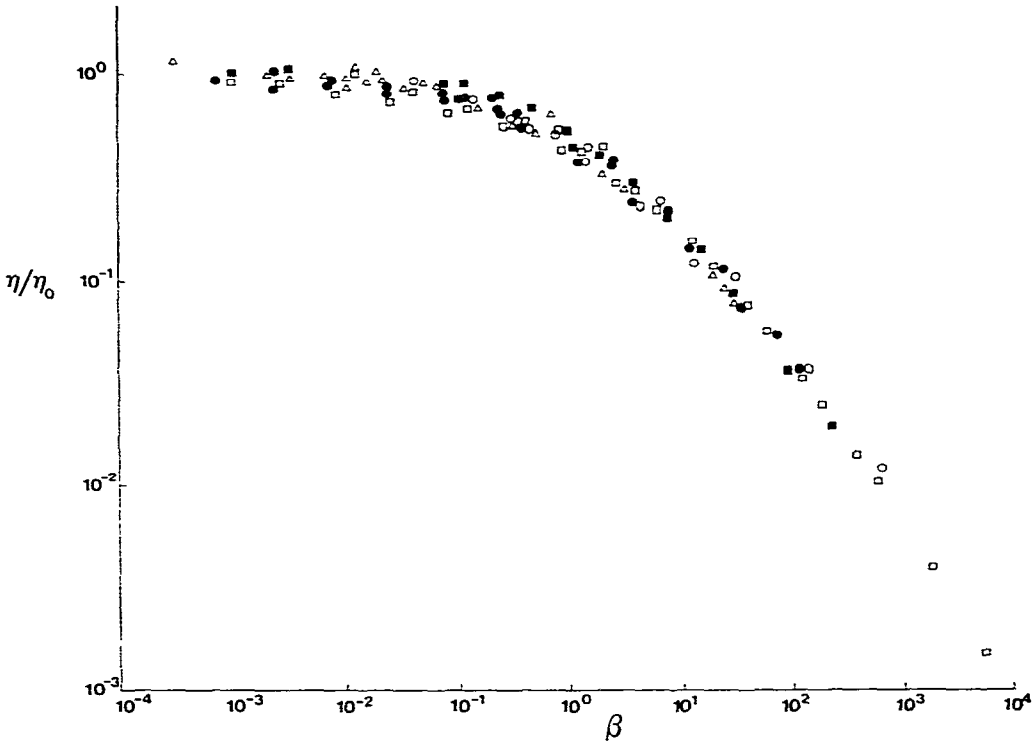

Fig. 10. Fractional decrease in viscosity with increasing, generalised shear-rate (β); symbols as in Fig. 8.

liquid-like. As the frequency of oscillation is increased, G′ increases faster than G″, crossing over at a frequency of ~20 rad.s^{-1}, from predominantly liquid-like behaviour in response to slow deformation, to predominantly solid-like response at higher frequencies. In Fig. 11, for the 1% solution, G″ is always greater than G′ in the frequency range measured (10^{-1}–10^2 rad.s^{-1}), whereas the 3% solution shows a cross-over at quite a low frequency, ~0.3 rad.s^{-1}. In Fig. 12, the data have been re-scaled, by dividing the moduli by concentration, and shifting horizontally along the relative frequency (ω_r) axis[8]. By combining the data for these different concentrations, the effective frequency range has been extended to cover seven decades.

CONCLUSIONS

The flow properties of guar galactomannan have been investigated over a range of concentrations for five samples of different molecular weight. From measured viscosities of the very dilute solutions, intrinsic viscosities were determined. By neglecting data for light-scattering intensities at low angles, reliable weight-average molecular weights were also determined, and Mark–Houwink parameters in the equation $[\eta] = K'M_r^a$ were evaluated; these were compared with other published

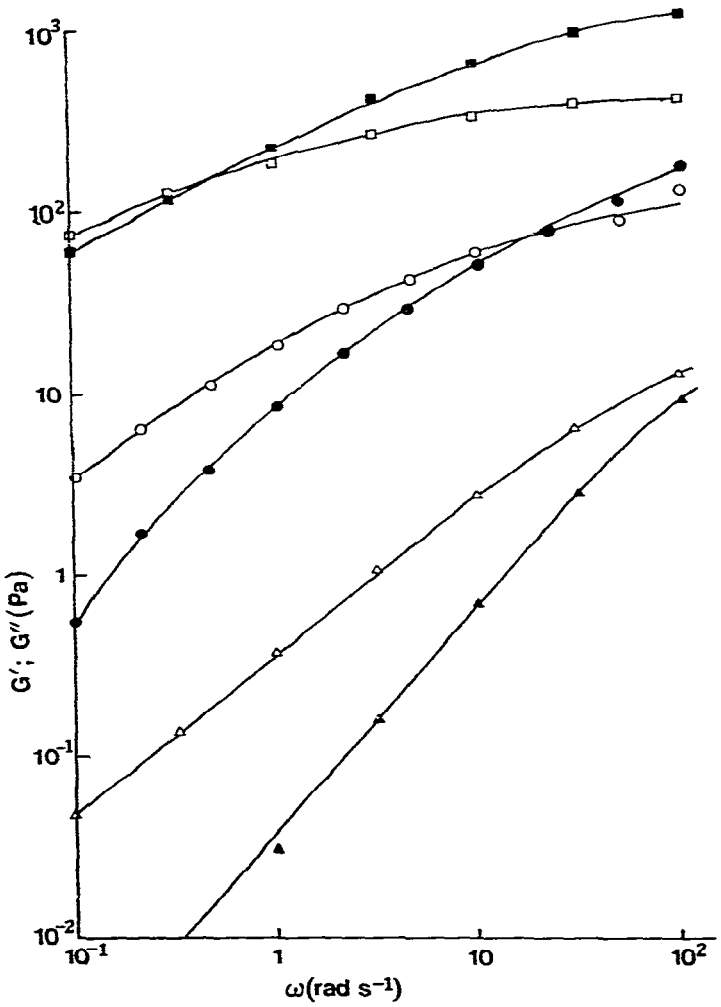

Fig. 11. Concentration dependence of solution viscoelasticity, illustrated for Vidocrem D: 1% (triangles), 2% (circles), and 3% w/v (squares). Filled symbols show the storage modulus (G′), and open symbols the loss modulus (G″).

values of K′ and α. From the Stockmayer–Fixman plot (Fig. 6), the intrinsic stiffness of the galactomannan backbone was estimated in terms of the characteristic ratio (C_∞). C_∞ was $\sim$12.6, which agrees well with results for carboxymethycellulose, which has a similar β-(1→4)-linked polymer backbone, and serves as a consistency check for our values of K′ and α. From the values of the Mark–Houwink parameters and of C_∞, we conclude that guar galactomannan behaves as a slightly stiffened, random-coil polymer in aqueous solution.

The increase in viscosity (η) with increasing concentration (c) of polymer becomes more pronounced above a critical concentration (c*) given, approximately, as $c^* \approx 4/[\eta]$ for all five samples ($4.5 \leqslant [\eta] \leqslant 12.5$). Below c*, the specific viscosity

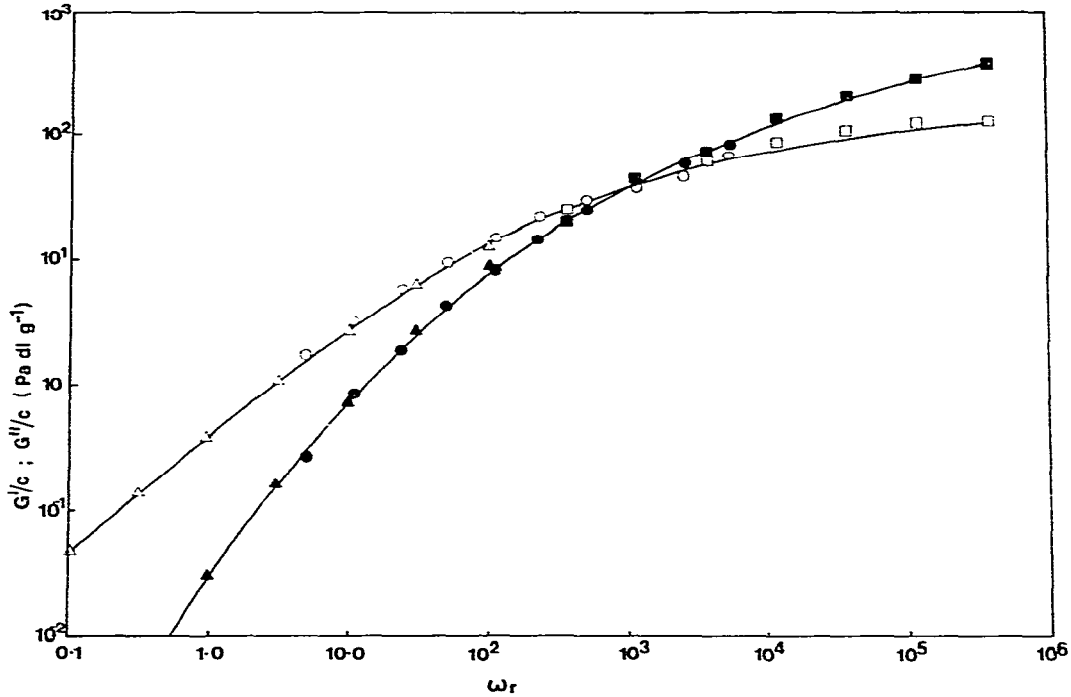

Fig. 12. Frequency–concentration superposition for the viscoelasticity data shown in Fig. 11, obtained (*a*) by dividing observed moduli by concentration, and (*b*) by a lateral shift of the data for the 2% and 3% solutions along the frequency axis. Reduced frequency (ω_r) is identical to applied frequency (ω) for the 1% sample. Symbols as in Fig. 11.

$\eta_{sp} \sim c^{1.3}$, whereas for $c > c^*$, $\eta_{sp} \sim c^p$, where the exponent p was found to be ~ 5.1, which is rather greater than is observed for polymers interacting purely by physical entanglement ($p \approx 3$–4), and suggests that more-specific polymer–polymer hyper-entanglements also contribute to the solution viscosity when $c > c^*$.

From the shear-rate dependence of viscosity, the effect of concentration and molecular weight upon the time-scale of entanglement coupling was also investigated. All of the data may be plotted on a single master curve, in terms of the dimensionless parameter $\beta[= \dot{\gamma}(\eta_0 - \eta_s)M_r/cRT]$, which may be derived from the bead-spring (Rouse) model of polymer dynamics. Data for the storage and loss moduli measured in oscillatory shear were also treated in a similar way, by dividing the moduli by c, and shifting the data laterally along the frequency axis. In this way, the effective range of oscillatory frequencies was extended to cover seven decades of time, and clearly illustrates the change in solution behaviour from predominantly liquid-like at low frequency to predominantly solid-like at the high-frequency (short time-scale) end of the mechanical spectrum. The generality of the response to change in the time-scale of deformation under both steady and oscillatory shear again supports our conclusion that guar galactomannan behaves as a random coil polymer.

ACKNOWLEDGMENTS

We thank Mr. A. J. Ingram, Mr. M. J. Izzard, Mr. R. K. Richardson, Mrs. L. A. Linger, and Mrs. S. A. Frangou for expert technical assistance, and Professor M. Bohdanecký, Dr. J. Kovář, and Dr. D. A. Rees for advice and discussions. We are also grateful for discussions with Dr. J. L. Doublier and Professor B. Launay, whose experimental results[3], over a narrower range of concentration, are in good agreement with our own.

REFERENCES

1 I. C. M. Dea and A. Morrison, *Adv. Carbohydr. Chem. Biochem.*, 31 (1975) 241–312.
2 R. L. Whistler, *Industrial Gums*, 2nd edn., Academic Press, New York, 1973.
3 J. L. Doublier and B. Launay, *J. Text. Stud.*, 12 (1981) 151–172.
4 J. L. Doublier and B. Launay, *Proc. Int. Congr. Rheology, Gothenburg, 6th*, 1976, pp. 532–533.
5 W. R. Sharman, E. L. Richards, and G. N. Malcolm, *Biopolymers*, 17 (1978) 2817–2833.
6 S. C. Naik, *Proc. Int. Congr. Rheology, Naples, 8th*, Vol. II, 1980, pp. 341–346.
7 W. W. Graessley, *Adv. Polym. Sci.*, 16 (1974) 1–179.
8 J. D. Ferry, *Viscoelastic Properties of Polymers*, 3rd edn., Wiley, New York, 1980.
9 E. R. Morris and S. B. Ross-Murphy, *Techniques in Carbohydrate Metabolism*, B310 (1981) 1–46.
10 E. R. Morris, D. A. Rees, E. J. Welsh, L. G. Dunfield, and S. G. Whittington, *J. Chem. Soc., Perkin Trans. 2*, (1977) 793–800.
11 E. R. Morris, A. N. Cutler, S. B. Ross-Murphy, D. A. Rees, and J. Price, *Carbohydr. Polym.*, 1 (1981) 5–21.
12 M. Dubois, K. A. Gilles, J. K. Hamilton, P. A. Rebers, and F. Smith, *Anal. Chem.*, 28 (1956) 350–356.
13 A. G. Ogston and J. E. Stanier, *Biochem. J.*, 53 (1953) 4–7.
14 H. Eisenberg and E. F. Casassa, *J. Polym. Sci.*, 47 (1960) 29–44.
15 W. Burchard and B. Pfannemüller, *Macromol. Chem.*, 121 (1969) 18–32.
16 K. A. Granath, R. Stömberg, and A. N. de Belder, *Staerke*, 21 (1969) 251–256.
17 K. R. Roberts, J. A. Torkington, M. Gordon, and S. B. Ross-Murphy, *J. Polym. Sci., Part C*, 61 (1977) 45–62.
18 P. Kratochvíl, in M. Huglin (Ed.), *Light Scattering from Polymer Solutions*, Academic Press, New York, 1972.
19 R. C. Jordan and D. A. Brant, *Macromolecules*, 13 (1980) 491–499.
20 B. Pfannemüller, H. Meyerhoffer, and R. C. Schulz, *Biopolymers*, 10 (1971) 243–261.
21 D. W. Tanner and G. C. Berry, *J. Polym. Sci., Polym. Phys. Ed.*, 12 (1974) 941–975.
22 J. G. Southwick, H. Lee, A. M. Jamieson, and J. Blackwell, *Carbohydr. Res.*, 84 (1980) 287–295.
23 M. Daoud and G. Jannink, *J. Phys. (Paris)*, 39 (1978) 331–340.
24 R. L. Cleland, *Biopolymers*, 9 (1970) 811–824.
25 H. Yamakawa, *Modern Theory of Polymer Solutions*, Harper and Row, New York, 1971.
26 W. Burchard, *Macromol. Chem.*, 42 (1960) 151–164.
27 W. H. Stockmayer and M. Fixman, *J. Polym. Sci., Part C*, 1 (1963) 137–141.
28 W. Brown and D. Henley, *Makromol. Chem.*, 79 (1964) 68–88.
29 D. A. Rees and W. E. Scott, *J. Chem. Soc., B*, (1971) 469–479.
30 W. H. Stockmayer, *Br. Polym. J.*, 9 (1977) 89–91.
31 J. Kovář, I. Fortelný, and M. Bohdanecký, *Macromol. Chem.*, 180 (1979) 1749–1760.
32 M. Bohdanecký, J. Kovář, and I. Fortelný, *Polymer*, 20 (1979) 813–817.
33 M. Bohdanecký and J. Kovář, personal communication.
34 P. G. De Gennes, *Nature (London)*, 282 (1979) 367–370.
35 T. E. Newlin, S. E. Lovell, P. R. Saunders, and J. D. Ferry, *J. Colloid. Sci.*, 17 (1962) 10–25.
36 W. W. Graessley, *J. Chem. Phys.*, 47 (1967) 1942–1953.